Mon. Not. R. astr. Soc. (1979) **189**, 801–816

Dielectronic satellite spectra for highly charged helium-like ions – V. Effect of total satellite contribution on the solar flare iron spectra

F. Bely-Dubau *Observatoire de Nice, B.P. 252, 06007 Nice Cedex, France*
A. H. Gabriel *Appleton Laboratory Astrophysics Research Division, Culham Laboratory, Abingdon, Oxfordshire*
S. Volonté *Département d'Astrophysique, Université de Mons, 7000 Mons, Belgium*

Received 1979 May 30; in original form 1979 March 19

Summary. For satellites of the type $1s^2nl$–$1s\,2pnl$ in Fe XXIV, wavelengths and intensities have been calculated for $n = 4$. Together with previous calculations for $n = 2$ and 3, these enable the wavelengths and decay rates to be scaled for higher values of n. The series up to $n = 11$ for satellites of the resonance line $1s^2$–$1s\,2p\ ^1P_1$, and up to $n = 16$ for satellites of the intercombination line $1s^2$–$1s\,2p\ ^3P_1$, have been derived. This leads to a good estimate for the contribution of satellites to the apparent wavelength shift, width, and intensity of the resonance line, and thus to a value of the correction factor α needed for deriving electron temperature from satellite/resonance line ratios, as described in Papers I and II in this series. Also obtained, from the sum of all the satellites, is a new value for the major contribution (~ 90 per cent) to the total dielectronic recombination rate. At typical flare temperatures of 20×10^6 K, this is greater by a factor of two than values obtained from earlier semi-empirical formulae.

1 Introduction

In this paper we limit our consideration to the process

$$\text{Fe XXV } 1s^2 + e \rightarrow \text{Fe XXIV } 1s\,2pnl. \qquad (1)$$

This process of dielectronic recombination can give rise to at least three distinct observable effects; (a) the emission of resolvable dielectronic satellite spectral lines, due to decay of the above Fe XXIV configuration, with $n = 2$ or 3; (b) an apparent broadening and strengthening of the resonance and intercombination lines of Fe XXV, due to the same transitions as the above, but with larger values of n; and (c) a contribution to the total recombination rate of Fe XXV to Fe XXIV due to the sum of the effects for all values of n.

Previous papers in this series have been concerned only with effect (a) above. Thus Gabriel (1972, Paper I) and Bhalla, Gabriel & Presnyakov (1975, Paper II) dealt with $n = 2$

transitions, while Bely-Dubau, Gabriel & Volonté (1979, Paper III) derived the $n = 3$ satellite spectra. The present paper extends these calculations to the $n = 4$ satellites. These are then used as a basis for extrapolation to high n, using approximate scaling theory. The complete set of data thus obtained can be used in order to derive the observed effects (b) and (c) above. The convergent series of satellites at high n lead to a contribution to both the resonance and intercombination line intensities. Since they are at slightly shifted wavelengths from the parent lines, there is also a broadening and asymmetry effect on these lines. Paper II dealt with the $n = 2$ satellite intensity relative to the resonance line, as a diagnostic for temperature. Since the high n satellites contribute to the apparent intensity of the resonance line, the corrections derived in the present paper are required in order to improve the accuracy of such temperature measurements.

Finally, the sum of all these satellites leads to an improved estimate of the dielectronic recombination rate for the ion Fe XXV. It should be remembered however that this is only that part that depends on the core transition $1 \rightarrow 2$. Although this is by far the largest contribution, there will be a further component from the core transitions $1 \rightarrow 3$ and higher.

In Papers I and II it was shown that for $n = 2$ satellites there are in general two excitation processes possible; dielectronic recombination, and inner-shell excitation of Fe XXIV. In Paper III it was shown that for the low densities of astrophysical plasmas, for $n = 3$ satellites the inner-shell excitation process can be neglected. This is even more true for $n \geqslant 4$. In the present paper, therefore, only the dielectronic process is considered for the excitation of these states.

Following Papers I and III, the relative intensity of a satellite line I_s to the resonance line I, can be expressed as

$$\frac{I_s}{I} = F_1(T_e) \times F_2(S), \tag{2}$$

where F_1 is a function of temperature and the satellite level

$$F_1(T_e) = 1.104 \times 10^{-12} \frac{E_0}{T_e} \exp\left[(E_0 - E_s)/kT_e\right], \tag{3}$$

and F_2 is a function only of the satellite level

$$F_2(S) = \frac{g_s A_r A_a}{(A_a + \Sigma A_r)}. \tag{4}$$

Here A_a and A_r are the autoionising and radiative decay rates, and the sum is over all possible final states. E_0 and E_s are the energies in eV of the resonance and satellite levels above the helium-like ion ground state, and g_s is the statistical weight of the satellite level. Note that I is now the intensity of the resonance line alone, excluding any unresolved satellites. $F_1(T_e)$ is a function mainly of T_e(in K). It depends on the satellite only weakly through the term E_s in the exponential. For most purposes it is adequate to take one value of $F_1(T_e)$ for all the $n = 2$ satellites, another value for $n = 3$, and then a further value for $n = 4$ to ∞.

2 Computations for $n = 4$ satellites

The method of calculating wavelengths and radiative transition probabilities was identical to that described in Paper III for the $n = 3$ satellites. The calculation using the SUPERSTRUCTURE program (Eissner, Jones & Nussbaumer 1974) was the same as that run in Paper III with the same configurations included, and was carried out in intermediate coupling. As

expected for high Z ions, the results showed that the strongest interactions take place within each complex, indicating that, for example, the 1, 2, 4 data are not significantly affected by the 1, 2, 2 or 1, 2, 3 complexes, where here a complex is a set of terms designated by a set of three principal quantum numbers.

The auto-ionization rates were determined using the Distorted Wave (DW) method of Eissner & Seaton (1972), initially in LS coupling. However, in the present case, owing to limitations in computer storage, only the 1, 2, 4 complex was included in the calculation. This avoids the generation of bound channels such as 1, 3, 3; 1, 3, 4; 1, 4, 4; which have a negligible effect on the required data. In order to check consistency between the DW auto-ionization data and the corresponding radiative data, the DW-generated bound state wave functions were checked against the corresponding LS wave functions, generated as a first step within SUPERSTRUCTURE. Intermediate coupling autoionizing rates then followed by application of the coupling coefficients derived from SUPERSTRUCTURE, as in Paper III.

The range and number of lines contributing to the stronger satellite is almost the same as for $n = 3$. However, since these results are for a somewhat different application, we reproduce in Table 1 data for only those satellite lines having significant intensities. A new key designation (1 to 28) has been used for these lines, to distinguish them from $n = 2$ and $n = 3$ satellites, which had letter codes and letter-and-number codes respectively.

The satellite intensities have been plotted against wavelength in Fig. 1 where it can be seen that they form two distinct groups, around the resonance and intercombination line wavelengths. This double grouping, which is not seen for $n = 2$, was already clearly evident by $n = 3$ (Paper III), and can be predicted to become more clearly defined for higher n (see later).

3 Theory for high n satellites

3.1 INTENSITIES

Equations (2), (3) and (4) give an exact description of the satellite intensities, and were used in Papers I, II and III for this purpose. Any attempt to scale to high n levels inevitably involves the derivation of approximations, or the grouping of levels, since otherwise the total number of J-levels in the satellite scheme becomes excessive. The trouble arises since equation (4) contains a branching ratio

$$\frac{A_a}{(A_a + \Sigma A_r)},$$

and that such ratios do not average properly over sets of levels. For a large number of levels with random A_a and A_r, it might be expected that the average branching ratio would approximate to the branching ratio of the average transition rates. However, this approximation breaks down if there are a significant number of levels where the ratio is systematically near zero. This will occur either for auto-ionizing forbidden terms, such as $1s\,2p^2\,{}^2P$ in pure LS coupling, or for high l terms where $A_a \to 0$. In the present work, we ignore the former since we consider high Z, high n cases in which LS coupling breaks down effectively. The case of high l we attempt to deal with by excluding such terms before averaging the remainder.

The early dielectronic recombination work by Burgess (1965) concentrated mainly on those ions in which the resonance transition involves a $\Delta n = 0$ transition. These ions, for which the total dielectronic recombination rate is very large, involve dielectronic levels with n of several hundred. The implicit assumption in the formalism presented, that the core

Table 1. Calculated data for the stronger $n = 4$ satellites. All lines with $F_2(S) \geq 1 \times 10^{12}\,s^{-1}$ have been included.

		J-J'	λ (Å)	A_r (10^{13} s^{-1})	ΣA_r (10^{13} s^{-1})	A_a (10^{13} s^{-1})	$F_2(S)$ (s^{-1})	Is/I (at 20.10^6K)	Key
$1s^2 4s$ - $1s2p4s$	^2S - $(^1P)^2P$	1/2-1/2	1.8504	43.75	43.98	0.232	4.59(12)	2.29(-3)	1
	$(^3P)^2P$	1/2-3/2	1.8550	0.114	0.350	1.08	3.43(12)	1.71(-3)	2
	^4P	1/2-3/2	1.8599	3.76	4.13	0.036	1.29(12)	6.42(-4)	3
- $1s2s4p$	- $(^1S)^2P$	1/2-1/2	1.8588	2.55	3.50	1.67	1.65(13)	8.22(-3)	4
$1s^2 4p$ - $1s2p4p$	^2P - $(^1P)^2S$	3/2-1/2	1.8502	40.78	45.82	0.517	9.10(12)	4.53(-3)	5
	- $(^3P)^2S$	3/2-1/2	1.8548	1.50	5.78	0.331	1.62(12)	8.07(-4)	6
	- $(^1P)^2P$	3/2-3/2	1.8507	44.93	46.90	0.458	1.74(13)	8.67(-3)	7
	- $(^3P)^2P$	3/2-3/2	1.8559	0.494	3.08	0.021	1.25(12)	6.23(-4)	8
	- $(^1P)^2D$	3/2-5/2	1.8509	45.71	47.77	0.78	4.41(13)	2.20(-2)	9
		1/2-3/2	1.8506	44.90	46.39	1.25	4.71(13)	2.35(-2)	10
	- $(^3P)^2D$	3/2-3/2	1.8595	3.53	8.09	0.81	1.28(13)	6.37(-3)	11
		1/2-3/2	1.8589	0.634	8.09	0.81	2.30(12)	1.15(-3)	12

- ^4S	1/2-3/2	1.8601	2.12	4.45	0.131	2.43(12)	1.21(-3)	13		
- ^4D	3/2-5/2	1.8602	3.52	3.96	0.35	1.70(13)	8.47(-3)	14		
	1/2-3/2	1.8605	1.62	2.00	0.088	2.74(12)	1.36(-3)	15		
- 1s2s4s	- $(^1S)^2S$	3/2-1/2	1.8626	0.73	1.53	0.89	5.38(12)	2.68(-3)	16	
		1/2-1/2	1.8620	0.54	1.53	0.89	4.01(12)	2.00(-3)	17	
$1s^24d$ - 1s2p4d	^2D - $(^1P)^2D$	5/2-5/2	1.8504	18.95	46.84	0.236	5.70(12)	2.84(-3)	18	
		3/2-5/2	1.8502	26.87	46.84	0.236	8.08(12)	4.02(-3)	19	
	- $(^1P)^2F$	5/2-7/2	1.8504	45.79	46.45	0.658	5.12(13)	2.55(-2)	20	
		5/2-5/2	1.8501	26.19	45.06	0.532	1.83(13)	9.11(-3)	21	
		3/2-5/2	1.8499	17.72	45.06	0.532	1.24(13)	6.18(-3)	22	
	- $(^3P)^2F$	5/2-7/2	1.8548	0.417	1.68	0.056	1.08(12)	5.38(-4)	23	
	- $(^3P)^4F$	5/2-7/2	1.8595	3.03	3.80	0.091	5.66(12)	2.82(-3)	24	
- 1s2s4p	- $(^1S)^2P$	5/2-3/2	1.8613	0.487	2.00	0.796	5.55(12)	2.76(-3)	25	
		3/2-1/2	1.8616	0.195	3.50	1.67	1.26(12)	6.27(-4)	26	
$1s^24f$ - 1s2p4f	^2F - $(^1P)^2G$	7/2-9/2	1.8497	45.90	46.36	0.048	4.79(12)	2.39(-3)	27	
		5/2-7/2	1.8496	41.28	46.07	0.509	3.65(12)	1.82(-3)	28	

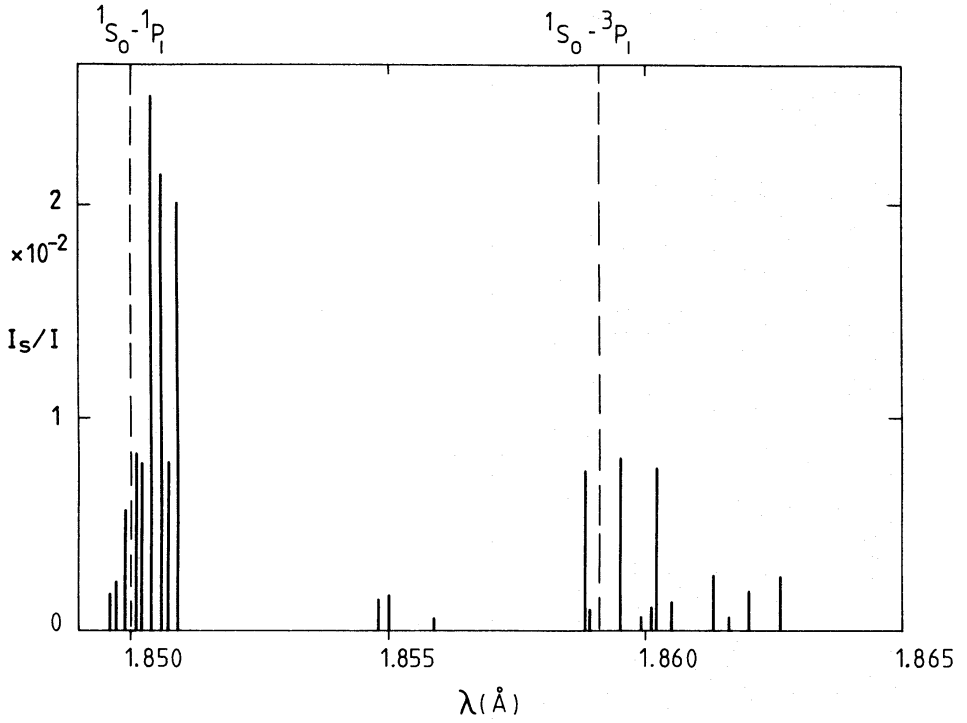

Figure 1. Wavelengths and relative intensities of the stronger $n = 4$ satellite spectra, at an electron temperature of 20×10^6 K.

coupling scheme is unperturbed by the outer hydrogenic electron orbital, is therefore valid. In this case, $F_2(S)$ becomes

$$2(2l + 1)g_{\text{res}} \frac{A_{\text{res}}A_{\text{a}}}{(A_{\text{a}} + A_{\text{res}})}. \tag{5}$$

Here A_{res} represents the transition probability of the resonance line, g_{res} the statistical weight of its upper level, and we have effectively grouped all the terms arising from the outer electron orbital *nl*. Burgess also points out that, for the cases considered, $A_{\text{a}} \to 0$ for all orbitals with l greater than about 8.

Shore (1969) considered the implication and limitations of this formalism, and pointed out that the A_{a} value used is in effect an average over all the terms based upon a coupling of the resonance level with the outer electron *nl*. He further pointed out that for the special case of ions with a resonance line $\Delta n = 1$ (i.e. the helium-like ion considered here) $A_{\text{a}} \to 0$ for l greater than about 2. In the present work we define such a maximum value of l as l_{max} and show that provided we consider only $l \leqslant l_{\text{max}}$ it is possible to make a valid grouping not only over *nl* but also over all l belonging to a single value of n and giving satellites to a single parent $^3P_1$ or $^1P_1$ (see below).

It is important to consider which core excitations in the $1s^2$–$1s\,2l'$ system will contribute to the satellite systems. From equation (5) it can be seen that when $A_{\text{a}} \ll A_{\text{res}}$, which will occur as n increases, $F_2(S)$ depends on A_{a} alone. Thus, any transition in the $1s^2nl$–$1s\,2l'nl$ system satisfying the condition $A_{\text{a}} < A_{\text{r}}$ for n in the range 10–15 is likely to produce a set of merged satellite lines. Satellites based upon the intercombination line $1s^2nl$–$1s\,2p\,(^3P_1)nl$ are in this category, in addition to the resonance line set $1s^2nl$–$1s\,2p\,(^1P_1)nl$, and must therefore be included. Satellites with core transitions $1s^2$–$1s\,2p\,^3P_2$ and $1s^2$–$1s\,2s\,^3S_1$ have values of A_{r} which are much smaller than A_{a}. The remaining levels $1s\,2s\,(^1S_0)nl$ and $1s\,2p\,(^3P_0)nl$ have no single-photon radiative decay permitted, in the limit of large n.

We have examined the detailed contributions arising from different nl in a Burgess-type dielectronic recombination calculation for a number of helium-like ion cases run by Summers (private communication). A number of factors emerged. Firstly, it is clear that a very good approximation is given by $l_{max} = 2$, independent of Z and n. This conclusion is confirmed by the present $n = 4$ calculations for iron, where it is seen that configurations with $l > 2$ (e.g. $1s\,2l'\,4f$) contribute less than 3 per cent to the total $\Sigma F_2(S)$ value.

The approximation adopted in the present work is therefore to group all terms for one n with $l \leqslant l_{max}$ for one parent to give

$\Sigma F_2(S) = F_2^1(n)$ for $^1P_1$ parent, or $F_2^3(n)$ for $^3P_1$ parent

$$= 2(l_{max} + 1)^2 g \frac{A\langle A_a\rangle}{(\langle A_a\rangle + A)} \tag{6}$$

where $l_{max} = 2$,

$$\langle A_a\rangle = \frac{\Sigma g_s A_a}{2(l_{max} + 1)^2 g}, \tag{7}$$

A is the transition probability of the parent resonance (or intercombination) line, and $g = 3$.

For $n = 3$ and $n = 4$ where complete calculations are available, it is possible to compare $F_2(n)$ derived as above with the more accurate sum $\Sigma F_2(S)$ over all lines for each n. This can be seen in the first two rows of Table 2. For $n = 4$, the error is only 1 per cent for the resonance satellites and 4 per cent for the (weaker) intercombination satellites, resulting in 1 per cent for the total. The approximation is expected to improve for higher n. Considering now only the n-totals, the errors are 8 per cent for $n = 3$ and 1 per cent for $n = 4$. The adoption of the approximate formula for $n = 5$ and above is therefore considered as justified, while the more complete calculations can be used for $n = 3$ and 4. Values of $\langle A_a\rangle$ for both resonance and intercombination satellites are now derived for $n \geqslant 5$ by scaling the $n = 4$ values, assuming them to have reached their asymptotic n^{-3} dependence. As shown in Table 2 this then leads to $F_2^1(n)$ and $F_2^3(n)$ values for higher n. It should be pointed out however that the above approximation may require further testing when applied to low Z ions, for which A_a may not always be less than A_r.

In Paper III it was pointed out that dielectronic levels with $n > 11$ have access to a new unpopulated continuum $1s\,2s\,^3S_1 + e$, and will tend to be destroyed by additional auto-ionization. This effect, which occurs above $n = 11$, is strictly true only for satellites to the $1s\,2p\,^1P_1$ parent. Satellites to the $1s\,2p\,^3P_1$ parent at slightly lower energy do not reach the $1s\,2s\,^3S$ threshold until after $n = 16$. Above these thresholds, equation (6) becomes modified by an additional large contribution to the $\langle A_a\rangle$ term in the denominator (loss term), but not in the numerator (dielectronic capture term). Although this decreases the contribution of the term significantly, it will not for a high Z ion like iron cut it off completely. To avoid calculating all these A_a rates to additional continua, we chose in this paper to cut off the contributions at $n = 11$ for the resonance series and at $n = 16$ for the intercombination series. In any case for helium-like ions in general most of the recombination, and therefore most of the satellite intensity, falls in the range of n between 2 and 10, with the upper limit decreasing for high Z. The maximum error thus introduced can be estimated by evaluating the contribution of the missing terms, ignoring the possibility of auto-ionizing to additional continua. From equation (6) we see that for $n \gtrsim 3$, $\langle A_a\rangle \ll A$ and varies as n^{-3}, so that $F_2(S)$ varies approximately as n^{-3}. The maximum error in total dielectronic rate, or satellite intensity ($n \geqslant 2$) due to this cut-off is then 2 per cent, while the maximum error in

Table 2. Comparison of approximate and detailed total line factors for the $n = 3$ and 4 shells, with extrapolated values for higher n. Approximate factors have been calculated using equation (6) with $A(^1P_1) = 4.633(14)$ and $A(^3P_1) = 3.823(13)$ s^{-1}. Values of $n^3\langle A_a\rangle$ for $n \geqslant 5$ have been assumed constant at their $n = 4$ values.

	Approximate Derivation					Detailed Calculation		
	$^1P_1$ Parent		$^3P_1$ Parent		Total	$^1P_1$ Parent	$^3P_1$ Parent	Total
n	$n^3\langle A_a\rangle$	$F_2^1(n)$	$n^3\langle A_a\rangle$	$F_2^3(n)$	$F_2^{1,3}(n)$	$F_2^1(n)$	$F_2^3(n)$	$F_2^{1,3}(n)$
3	3.37(14)	6.57(14)	1.02(14)	1.86(14)	8.43(14)	6.06(14)	1.71(14)	7.79(14)
4	2.73(14)	2.28(14)	1.20(14)	9.66(13)	3.25(14)	2.30(14)	9.27(13)	3.23(14)
5	"	1.18(14)	"	5.06(13)	1.69(14)			
6	"	6.81(13)	"	2.96(13)	9.77(13)			
7	"	4.29(13)	"	1.87(13)	6.16(13)			
8	"	2.89(13)	"	1.26(13)	4.15(13)			
9	"	2.02(13)	"	8.86(12)	2.91(13)			
10	"	1.47(13)	"	6.47(12)	2.12(13)			
11	"	1.11(13)	"	4.86(12)	1.60(13)			
12	-	-	"	3.75(12)	3.75(12)			
13	-	-	"	2.95(12)	2.95(12)			
14	-	-	"	2.36(12)	2.36(12)			
15	-	-	"	1.92(12)	1.92(12)			
16	-	-	"	1.58(12)	1.58(12)			

Table 3. Intensities of satellites to the resonance and intercombination lines, expressed as a proportion of the resonance line intensity, for $T_e = 20 \times 10^6$ K. The last column represents the sum of the two components (not separable for $n = 2$). The n-totals for $n = 2$, 3 and 4 have been derived from the complete calculations, whereas for $n \geqslant 5$ the approximate expression has been used (see Table 2).

n	$F_1(T_e)$	$\Sigma I_s(^1P)/I_{res}$	$\Sigma I_s(^3P)/I_{res}$	$\Sigma I_s/I_{res}$
2	1.20(-15)			1.641
3	6.27(-16)	0.38	0.107	0.487
4	4.98 (-16)	0.115	0.045	0.160
5	4.44(-16)	0.052	0.022	0.074
6	4.20(-16)	0.029	0.012	0.041
7	4.059(-16)	0.017	0.0076	0.0246
8	3.971(-16)	0.011	0.0050	0.0160
9	3.913(-16)	0.008	0.0035	0.0115
10	3.871(-16)	0.006	0.0025	0.0085
11	3.841(-16)	0.004	0.0019	0.0059
12	3.818(-16)	-	0.0014	0.0014
13	3.800(-16)	-	0.00112	0.00112
14	3.786(-16)	-	0.00089	0.00089
15	3.775(-16)	-	0.00072	0.00072
16	3.766(-16)	-	0.00060	0.00060
Total				2.474

the satellite contribution to the resonance line intensity ($n \geqslant 3$) is 5 per cent of that contribution. The actual errors are expected to be substantially less than these.

The data in Table 2 can be converted into satellite line intensities by multiplying by $F_1(T_e)$. However, errors will be introduced unless account is taken of the change of $F_1(T_e)$ with n, at least for $n = 2$, 3 and 4, where most of the satellite intensity contribution occurs. For $n \geqslant 4$ it is adequate to approximate $(E_0 - E_s)$ in equation (3) by the hydrogenic expression

$$\frac{13.6(Z-2)^2}{n^2} \text{ eV}.$$

Table 3 lists $F_1(T_e)$ for a typical flare temperature of 20×10^6 K, where it can be seen to change by more than a factor of 3 as n increases. Also shown in Table 3 are the resulting satellite intensities and their total.

3.2 WAVELENGTH DISTRIBUTION

In the above we derived expressions for the intensities of the satellites for each value of n, together with calculated wavelengths for $n = 2$, 3 and 4. In this section we derive approximations to give, in effect, the wavelength distributions of the satellites with $n \geqslant 5$.

First it is necessary to reconsider the tendency of the $n = 3$ and 4 satellites to fall into two wavelength groups. Examination of Fig. 1 and Table 1 shows that the group around the

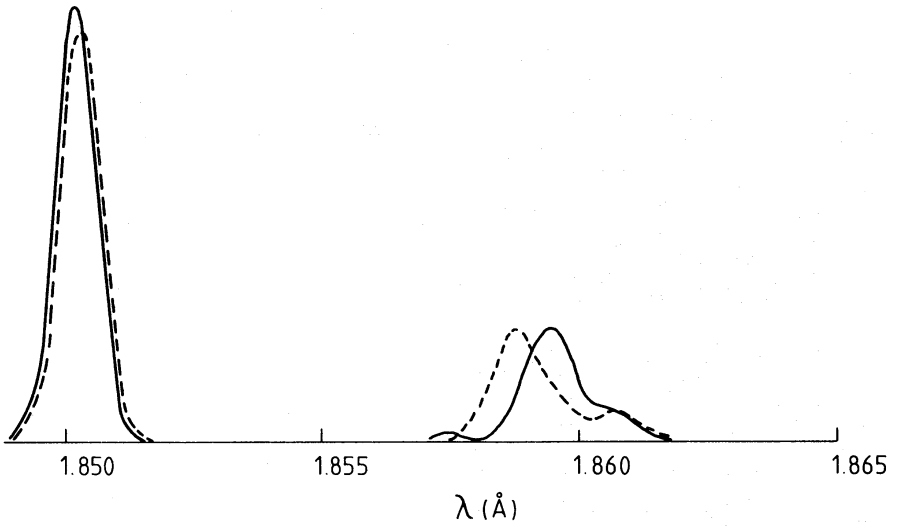

Figure 2. Intensity distribution for $n = 5$ satellites at a Doppler temperature of 20×10^6 K, derived by scaling from $n = 4$ spectra (solid line), and $n = 3$ spectra (broken line).

resonance line is based entirely on satellite terms having a (^1P) parentage, while that around the intercombination line arise mostly from (^3P) parents, with a small number from (^1S) parents. Asymptotic theory (Section 3.1) predicts high n series converging onto the two lines (resonance and intercombination) only. It would appear that the apparent (^1S) parents in

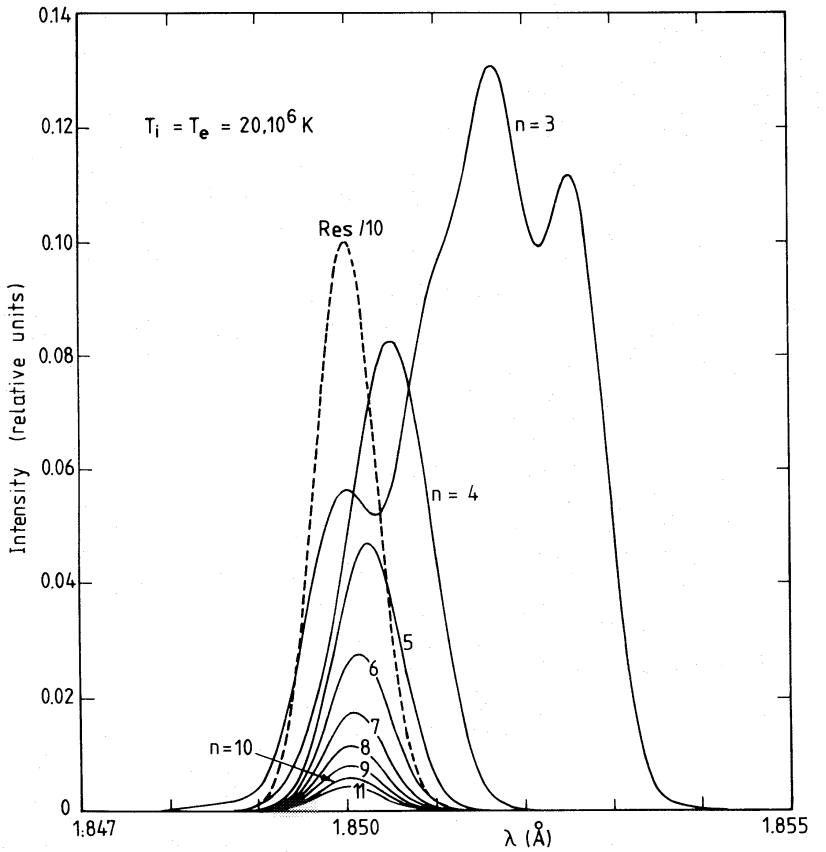

Figure 3. Satellites to the resonance line, showing the contribution from each shell, at electron and Doppler temperatures of 20×10^6 K.

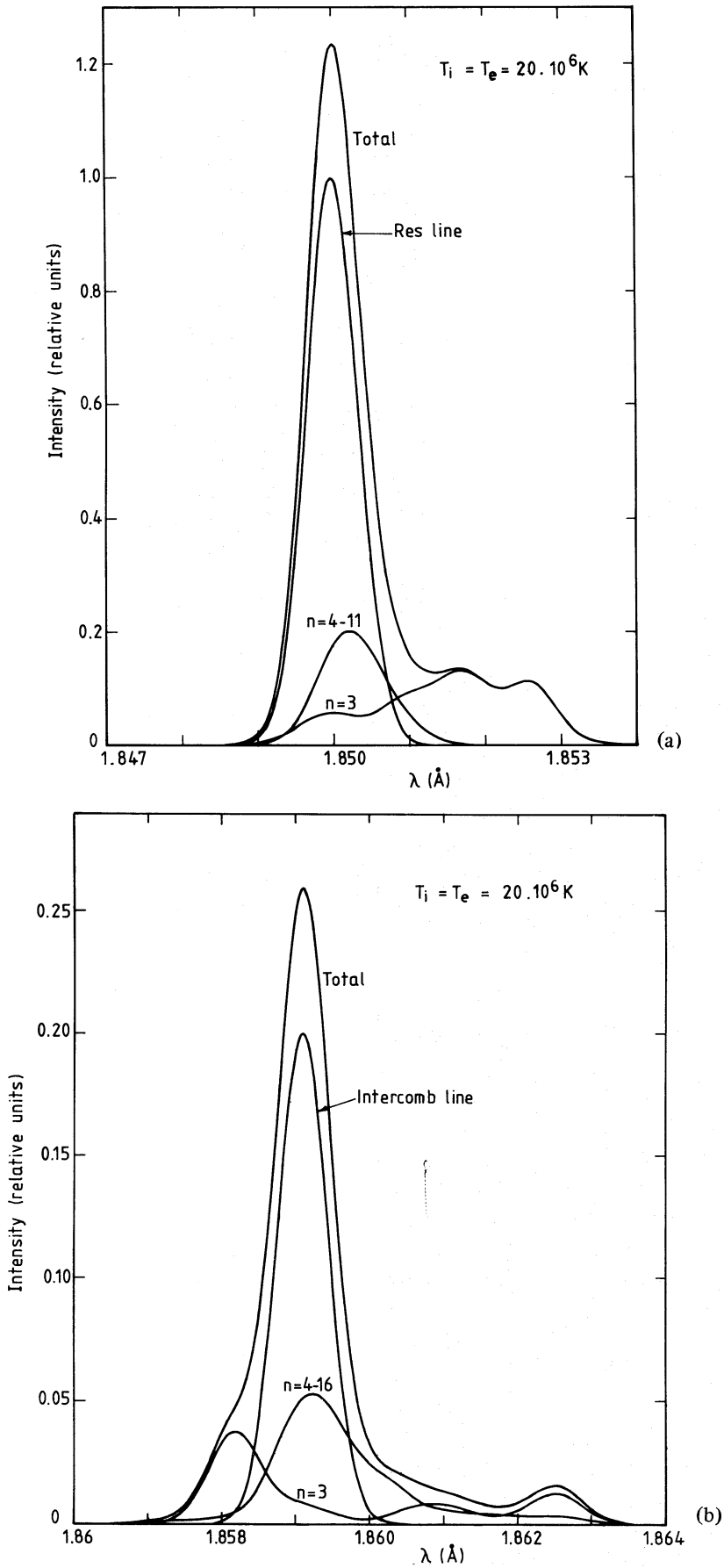

Figure 4. Total spectrum close to the resonance line (a), and the intercombination line (b). The effect of satellites on the shift, breadth and intensity of the apparent resonance line is clearly shown. The intercombination feature does not include the effect of nearby $n = 2$ satellites. Spectra are normalized to the peak intensity of the resonance line.

Table 4. Contribution within ± 0.001 Å of the resonance line of all satellites, expressed as a function of the resonance line intensity.

T (10^6K)	(Satellite contribution)/I (α)	Correction factor ($1+\alpha$)
5	4.55	5.55
7	2.08	3.08
10	1.06	2.06
15	0.564	1.564
20	0.379	1.379
30	0.227	1.227
40	0.162	1.162
50	0.125	1.125
60	0.102	1.102
70	0.086	1.086
80	0.075	1.075
90	0.066	1.066
100	0.059	1.059

Table 1 have intensity mainly due to a certain parentage mixing in the satellite levels, and this is an effect that vanishes asymptotically at high n. We are therefore justified in assuming that for $n = 5$ and above, only the two convergent groups remain and that these are based upon ($^1P_1$) and ($^3P_1$) parentages.

Asymptotically for high n, the energy (or wavelength) difference between each satellite and its parent line can be represented by terms which all vary as n^{-3}. Furthermore, the auto-ionization rate A_a for each line will also vary as n^{-3}. Once $A_a \ll A_r$ for a line, its intensity from equation (4) will vary as A_a, and thus as n^{-3}. We therefore propose as an approximation that the intensity distribution pattern for each of the two groups, for each n, be considered as constant for $n \geqslant 4$, when measured on a wavelength scale $n^3\Delta\lambda$, where $\Delta\lambda$ is the wavelength interval to the appropriate parent line. This approximation, which may be poor for individual satellite lines, becomes more valid when it is realized that for $n = 5$ and above, convolution of the spectrum with a thermal Doppler broadening has a marked smearing effect, so that only the general intensity distribution in the group remains. As a severe test of this approximation, Fig. 2 shows the $n = 5$ satellite spectrum deduced in this way from the $n = 4$ spectrum (full line) and also from the $n = 3$ spectrum (dashed line), taking a Doppler temperature, T_i, of 20×10^6 K. The area under each of the two groups has been normalized to relate to the total intensities from Table 3. Fig. 2 shows that the asymptotic limit in the above approximation has been effectively reached for the resonance group by $n = 3$, although the situation is not as good for the intercombination group. We now make the assumption that the $n = 4$ satellites are a good asymptotic representation for both groups, and use these as a basis for deriving the shapes of the groups for each higher n, while normalizing the intensities to the corresponding values in Table 3.

Fig. 3 shows the contribution for each n for members of the resonance group of satellites, computed for values of both T_e and T_i of 20×10^6 K. Note that above $n = 7$ or 8 the shape is determined almost entirely by the thermal Gaussian. Fig. 4(a) shows the effect of summing

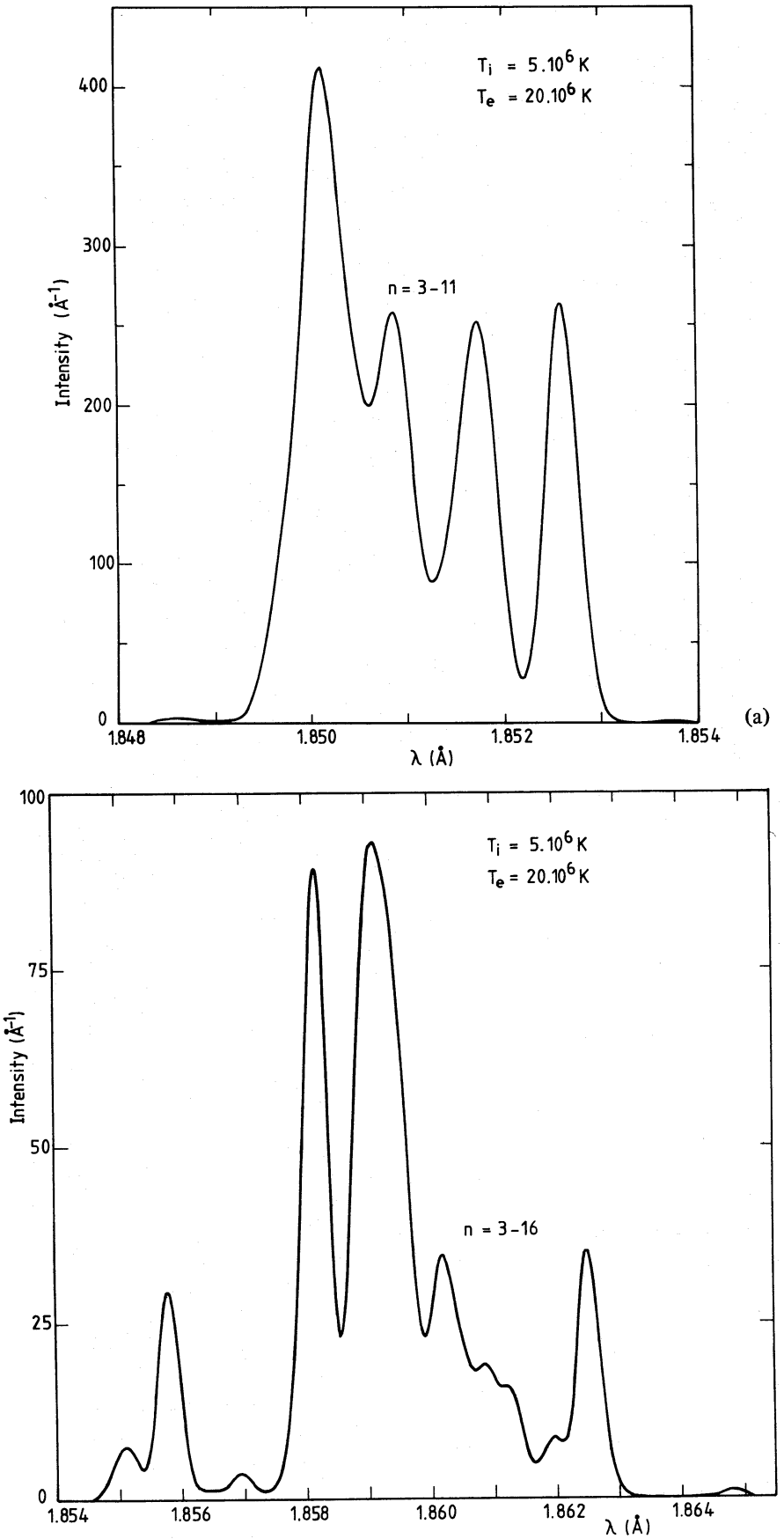

Figure 5. Satellite spectra for $n \geqslant 3$ at a Doppler temperature of 5×10^6 K and electron temperature of 20×10^6 K, for resonance line feature (a) and intercombination line feature (b). Spectra are normalized to unity for the area under the true resonance line profile (not shown).

over all n from 3 to 11. Note that the presence of the satellites has the effect of increasing the apparent intensity of the resonance line by 22 per cent in peak height, by 10 per cent in width and by 38 per cent in area if we include intensity out to ±0.001 Å. A similar plot for the intercombination line group is shown in Fig. 4(b). In this case it has been necessary to make an assumption for the intensity of the intercombination line $^1S_0$–$^3P_1$, which has been taken as 0.20 of the resonance line intensity, as in Paper I.

We are now in a position to calculate the total effective satellite contribution to the apparent resonance line intensity, as a function of temperature. Keeping to the same definition as above, i.e. all intensity within ±0.001 Å of the resonance line, it is necessary to include 33 per cent of the $n = 3$ intensity plus all of the $n = 4$ to 11 resonance satellite group. This factor is listed in Table 4. This is then the intensity correction factor α referred to (but incorrectly estimated) in Papers I and II. The treatment in Papers I and II resulted in a zero value of α for iron. Before deriving temperatures from the data in Papers I and II or III, the calculated satellite/resonance line ratios should first be divided by the factor $(1 + \alpha)$ listed in Table 4.

In order to assist the reader in predicting the appearance of the higher satellites for other values of T_e and T_i, Fig. 5(a) and (b) shows the combined satellite structure for $n = 3$ up to the cut-off value, for $T_e = 20 \times 10^6$ K and a very low value of T_i of 5×10^6 K. To obtain the distribution for any higher value of T_i, it is only necessary to convolve the curves of Fig. 5 with a Gaussian equivalent to a temperature of $(T_i - 5 \times 10^6\,\mathrm{K})$. The intensity axes of Fig. 5 are normalized so that the areas under the curves are correct for a resonance line of area unity at a value for T_e of 20×10^6 K. Although the temperature variation functions $F_1(T_e)$ are different for each value of n, a good approximation can be obtained by using the values appropriate to $n = 4$ or 5, in order to scale the intensities of Fig. 5, for electron temperatures other than 20×10^6 K.

4 Dielectronic recombination

The total rate of dielectronic recombination is simply the sum of total intensity in photons of all the satellite lines. From Paper I we can obtain a recombination rate

$$R_d = \frac{2.06 \times 10^{-16}}{T_e^{3/2}} \Sigma \exp(-E_s/kT_e) F_2(S) \tag{8}$$

which rewritten in terms of $F_1(T_e)$ becomes

$$R_d = \frac{1.873 \times 10^{-4}}{E_0 T_e^{1/2}} \exp(-E_0/kT_e) \Sigma F_1(T_e) F_2(S). \tag{9}$$

If the summation is carried out over all the satellites considered here from $n = 2$ up to the cut-off we then have the total dielectronic rate due to the core excitation 1 to 2, i.e. due to

$1s^2 + e \rightarrow 1s\,2lnl'$.

This total is shown as the solid curve in Fig. 6. The lowest terms missing from this summation are of the type $1s\,3l\,3l'$, and are reduced in effective contribution by a number of factors, including the fact that all of them have alternative continua of the type $1s\,2l + e$ into which they can auto-ionize. An estimate can be made of the contribution of these terms, which are about 10 per cent of the above total. The curve in Fig. 6 is therefore ~ 90 per cent of the total dielectronic recombination rate for the ion. For comparison, we show dotted in Fig. 6 the values obtained using Burgess' (1965) semi-empirical formula, evaluated for core excitations up to $n = 5$. The Burgess values are low at low temperatures due to the neglect of the energy difference $(E_0 - E_s)$.

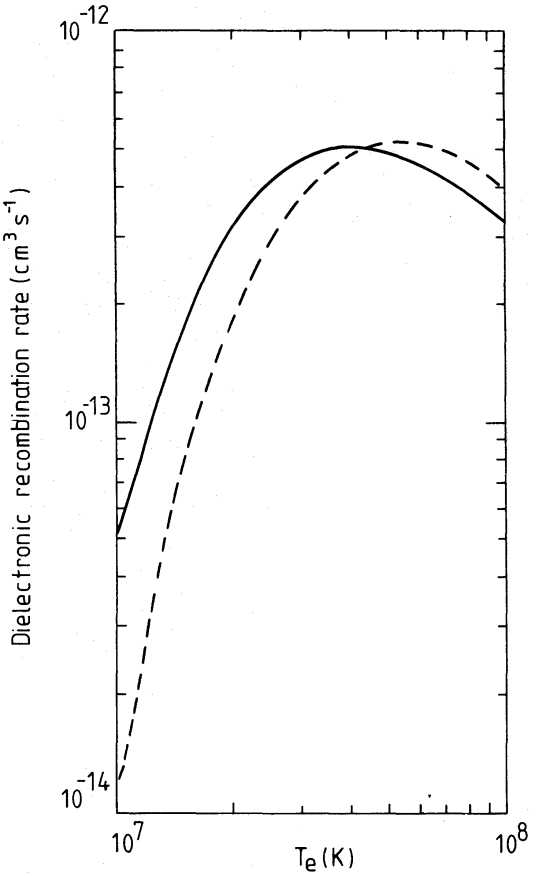

Figure 6. Dielectronic recombination rate as a function of temperature. The solid line represents the sum of all resonance and intercombination satellites from the present work. The broken line is from the semi-empirical formula of Burgess (1965).

5 Conclusions

Theory for the wavelengths and intensities of dielectronic satellites to helium-like iron spectra has been extended to $n = 2$, 3 and 4. Using these, extrapolation procedures have been developed to enable approximate values to be obtained for higher values of n.

The influence of these satellites on the appearance of the spectra can now be evaluated, including the apparent shift and broadening of the resonance line. Correction factors for the resonance line intensity have been obtained which should be used in conjunction with the earlier Papers II and III. Using this theory, improved values have been obtained for the major contribution to the dielectronic recombination coefficient for Fe XXV to Fe XXIV.

The theory developed is crucial for the interpretation of high resolution spectra of solar flares, to be obtained using the X-ray Polychromator on board the *Solar Maximum Mission* satellite, due for launch towards the end of 1979. Unfortunately, existing solar flare X-ray spectra are of insufficient quality to justify application of the results in the present paper.

6 Acknowledgments

The authors are grateful to Drs J. Dubau and W. Eissner for many helpful discussions during the course of this work. Thanks are also due to Mr J. Lion for assistance with some of the computations.

References

Bely-Dubau, F., Gabriel, A. H. & Volonté, S., 1979. *Mon. Not. R. astr. Soc.*, **186**, 405 (Paper III).
Bhalla, C. P., Gabriel, A. H. & Presnyakov, L. P., 1975. *Mon. Not. R. astr. Soc.*, **172**, 359 (Paper II).
Burgess, A., 1965. *Astrophys. J.*, **141**, 1588.
Eissner, W., Jones, M. & Nussbaumer, H., 1974. *Comp. Phys. Comm.*, 8, 270.
Eissner, W. & Seaton, M. J., 1972. *J. Phys. B.*, **5**, 2187.
Gabriel, A. H., 1972. *Mon. Not. R. astr. Soc.*, **160**, 99 (Paper I).
Shoré, B. W., 1969. *Astrophys. J.*, **158**, 1205.